Smart Agricultural Technology 12 (2025) 101205

Contents lists available at ScienceDirect

Smart Agricultural Technology

journal homepage: www.journals.elsevier.com/smart-agricultural-technology

Evaluating the automated measurement of abnormal rising and lying down behaviours in dairy cows using 3D pose estimation

Adrien Kroese [a,*], Niclas Högberg [a], Elena Diaz Vicuna [b], David Berthet [c], Nils Fall [a], Moudud Alam [d], Lena-Mari Tamminen [a]

[a] Department of Clinical Sciences. Faculty of Veterinary Medicine and Animal Science, Swedish University of Agricultural sciences, Ulls väg 26, 756 51 Uppsala, Sweden
[b] Università degli Studi di Torino. Department of veterinary science, Largo Paolo Braccini 2 10095 Grugliasco, Italy
[c] Sony Sweden, Filial to Sony Europe Ltd. (UK), Mobilvägen 221 88 Lund, Sweden
[d] School of Information and Engineering, Dalarna University, Högskolegatan 2, 791 88 Falun, Sweden

ARTICLE INFO

Keywords:
Animal welfare assessment
Free-stall cubicle
3D pose estimation
Rising behaviour
Lying down behaviour
Precision livestock farming

ABSTRACT

The structure of cubicles can hinder cows' movements when transitioning between postures, leading to atypical motion patterns. Assessing posture transitions relies on visual observations. This study presents a framework for complementing these assessments with kinematic measurements using 3D pose estimation. A total 809 rising and 791 lying down posture transitions were recorded over 12 cubicles by 7 synchronized cameras and processed with 3D pose estimation locating the position of the poll, withers, T13 and sacrum. First, the displacement of the keypoints was used to detect phases of the posture transitions. This detection was compared with visual observations of 200 recordings. The average mean absolute difference in detected timestamps between human and machine across all phases was 0.5 s (average $\sigma = 0.7$) and was under 0.9 s for all phases. Second, indicators were scored based on spatial use and duration, and their distribution compared to existing thresholds. We observed that 59.9 % of rising bouts and 29.1 % of lying down bouts exceeded at least one threshold. Rising delay occurred in 2.8 % of rising bouts and backwards crawling in 59.2 %. Lying down duration exceeded the threshold in 28.9 % of bouts, and rear limbs shifting duration in 8.3 %. Side lunge had a binary threshold which was not adapted to continuous sensor data. Finally, we investigated the association between indicators and found distinct dimensions for head lunge and crawling. We conclude that 3D pose is useful to score posture transition indicators, and that several indicators should be used together to capture distinct dimensions.

1. Introduction

Free stall cubicles are designed to encourage cows to lie down rather than stand, and to defecate outside of the bed. Balancing design elements involves a trade-off at the expense of movement opportunities. For instance, neck rails improve hygiene but increase the incidence of abnormal movements [1]. The ability for cows to comfortably transition between postures is an important parameter of cow comfort in stalls [2,3].

The ability to perform unhindered posture transitions, such as getting up and lying down, is recognized as a critical component of cow welfare and resting [4,5]. Sufficient space and stable footing are needed to perform these transitions smoothly [6]. It has been hypothesised that the ability to comfortably transition between postures promotes the occurrence of lying behaviour [7]. Adequate rest – in terms of duration, frequency and comfort – is important to dairy cows, studies having shown that cows will work to access resting spots [8]. Brouwers et al. [4] found that in cubicles with flexible dividers, which allow for a more ample movements, cows lied down more frequently and that daily lying duration was higher, suggesting that the ability to lie down without obstruction promotes resting behaviour.

Comfortably transitioning between postures extends beyond physical health, these movements are linked with behavioural expressions of comfort and well-being [5]. Cows that struggle with these transitions may experience increased stress and discomfort, which can affect their overall behaviour and productivity. Providing an environment that facilitates posture transitions can lead to increased resting, and to improved welfare outcomes [9,10]. The quality of posture transition movements is used as a welfare assessment indicator, reflecting the comfort offered by the stall [6,11,12].

* Corresponding author.
E-mail address: adrien.kroese@slu.se (A. Kroese).

https://doi.org/10.1016/j.atech.2025.101205
Received 17 November 2024; Received in revised form 14 July 2025; Accepted 14 July 2025
Available online 18 July 2025

In practice, the assessment of posture transition comfort is typically performed visually by a trained assessor, scoring indicators associated with adverse welfare outcomes, such as bumping the head on the cubicle bars [12]. The Welfare Quality assessment framework contains 2 criteria which are the duration of standing-to-lying (STL) posture transitions and collisions with equipment [11]. The Swedish framework Fråga Kon (Växa, Stockholm, Sweden), which is meant as a practical on-farm assessment of welfare through animal-based measures, assesses the quality of lying-to-standing (LTS). Visual evaluation has limitations, mainly low observation frequency, the inability to re-evaluate when scoring live, and the need for the observer to note various behaviours which may occur simultaneously. Observer disagreement does not seem to be a major risk however; for instance Zambelis et al. [12] reported a Kappa of 0.93 at its lowest when assessing abnormal posture transition indicators. The assessment frameworks presented earlier rely on few or single quantitative indicators for each posture transition.

Precision livestock farming (PLF) technology offers an opportunity to monitor posture transition movements continuously, simultaneously and objectively, and to automatically detect abnormalities in posture transitions.

Sensors have already been used to assess posture transitions. Motion capture has been applied to measuring head lunge (the forward displacement of the head) and showed that cows in open packs lunged further when lying down by a mean of 6 cm while using the same total longitudinal space [13]. Motion capture is a gold standard for kinematic measurements of animals [14] but remains impractical in production settings, which may explain the low sample size ($n = 5$) in the former study [13]. Brouwers et al. [15] developed a machine learning model to detect abnormal lunge movements from accelerometer data. They used annotations by trained observers of the occurrence of abnormal lunges as labels and tri-dimensional acceleration features as input. The accuracy of their model reached up to 74 %, with the class having the highest accuracy being backwards crawling. This metric is encouraging but needs refining for practical implementation. It is important to note that this result is unlikely due to limitations in the model. Rather, the training labels were annotated using ethograms developed for visual observations, in which the same behaviour class can be reflected by vastly different motion patterns [15].

A possible technology to assess kinematic features during posture transitions is pose estimation [16]. A widespread example of applications of pose estimation in detecting bovine kinematic abnormalities is lameness assessment [17,18]. Pose estimation will track the displacement of key anatomical features to quantify indicators of abnormal locomotion [19]. Kinematic assessment with 2D pose estimation, as is commonly done to assess lameness [19–21] relies on straight walks along an assigned path, perpendicular to the camera's line of sight [17]. Such setup with a fixed orientation of the camera is not feasible for assessing posture transitions of several animals in a production setting. The challenge is that the angle between a single camera's field of view and each stall varies with the stall location, distorting joint angles and perspectives. Pose estimation fusion in 3D from multi-view computer vision however is invariant to camera placement [22] and thus offers more flexibility, when sensor placement is constrained by the existing barn design. Importantly for practical application, pose estimation does not rely on markers (unlike motion capture) and applies to all subjects in the scene (all cows in the cubicles being filmed).

From the state-of-the art in visual assessment there are two challenges that sensor-based posture transition assessment could overcome; the difficulty in scoring multiple indicators in a single event and the time needed to assess regularly. We thus propose a method to identify the phases of posture transitions using multi-view fusion of pose estimation in 3D, and detect the occurrences of abnormalities.

The aim of the study was (i) to develop a method to detect successive phases of cows' posture transitions from 3D poses and score comfort indicators during these phases, (ii) to validate the detection against the human eye and assess its robustness to noisy data and (iii) to study the distribution and possible association of posture transition indicators. To do so, we used a Sony multi-camera system (Sony Sweden, Lund, Sweden) to generate 3D poses of dairy cows in a free stall barn during both posture transitions. Using the 3D pose, we detected the different phases of the posture transitions using change-point detection and supervised learning to then compare the detected timestamps to those annotated by human observers. Then, we measured the duration of each phase as well as kinematic features to identify bouts with indicators exceeding thresholds for comfortable movements. Finally, we investigated whether there existed an association between indicators.

2. Materials and methods

In this study, we use 3D pose to measure indicators of posture transition quality. Here is a general overview: video sequences showing posture transition bouts were recorded with synchronized cameras with overlapping fields of view. The multi-camera system was calibrated to determine intersecting lines of sight. The 3D pose of cows was inferred from 2D poses estimated on synchronized frames across several cameras. The displacement of anatomical features of cows was tracked throughout bouts and the timestamp of specific phases was detected and compared with manual annotations. Finally, kinematic indicators of posture transition were measured and compared to existing thresholds.

2.1. Location and animals

2.1.1. Study area

Video recordings from 7 cameras (G3 Bullet, Ubiquiti) were collected on 30 separate days between 2021 and 12–08 and 2022–04–28 at all times of day and night. The cameras were placed around an area of a free-stall barn covering 12 stalls (Cubicle divider cc1800 with rigid head bar, Delaval International, Tumba, Sweden) located next the sorting gate of the automatic milking system (VMS 300, DeLaval International, Tumba, Sweden). The cameras were installed around the rows of stalls, between 2.8 and 3.6 m high, and oriented towards the rows of cubicles so that all cubicles in the study ward, including forward lunge room defined as the 60 cm beyond the head rail, were visible by at least 2 cameras. All recordings were obtained at the Swedish Livestock Research Centre's dairy barn (Uppsala, Sweden).

2.1.2. Animals

The herd comprises Swedish Holstein and Swedish Red cattle housed indoors during the study period but with pasture access between May and September. On average, 51 lactating cows were present simultaneously in the pen, with individuals being added and removed throughout, for a total of 183 different individuals having visited the pen during the study period. The average parity of the animals at the start of data collection was 2 with a mode of 1. Days since calving ranged from 6 to 447 with an average of 149. 7 animals were diagnosed with non-reproductive health disorders during the study. Specifically, 3 cows were treated for mastitis, 1 cow was identified with severe lameness, 1 cow with a hoof inflammation, and 2 cows were diagnosed with paresis. Average individual body condition score as measured by the BCS camera (BCS, DeLaval International, Tumba, Sweden) during the trial was 3.4 ± 0.33 ($\mu \pm \sigma$).

Cows are milked robotically with voluntary access up to 12 h until which they are brought to milking if they have not gone voluntarily. Passage through the milking robot's sorting gate is necessary to access feed. Cows underwent claw health inspection and trimming every 6 months

2.2. 3D pose estimation

This study employs a synchronized multi-camera system (Sony Sweden) with known intersecting lines of sight to reconstruct 3D poses from 2D key-point estimates. Each pose comprises the coordinates of

anatomical landmarks (head at the poll, highest point of the withers, T13, and sacrum at the uppermost point of the ilium) in an arbitrary coordinate system at a given timestamp. HRNET [23] is used to estimate key-points in 2D for each frame. These poses are then fused to obtain 3D key-points.

Frames are synchronized by reading the frame timestamp in the metadata and using the first frame with a common full second transition as frame 0. Synchronization is maintained throughout the recording of up to 35 s by reading the frame order of arrival in the processing buffer for each camera, recording at the same framerate. The 3D fusion of poses is robust to misalignments of up to 0.5 s for movements corresponding to the velocity of a human walking.

Intrinsic calibration parameters are determined using structure-from-motion algorithm [24]. This step determines the cameras' distortion parameters and ensures alignment of all cameras' origin and axes with world coordinates [25]. Then, the system was extrinsically calibrated to determine intersecting lines of sight between cameras using the technique described by Moliner et al. [26]. A single human is tracked by the pose estimator through the area of interest (twelve cubicles and they alley between them or a surface area of 7.5×6.4 m). A preliminary 3D pose of the human is determined by triangulating each unique key-point across 2D poses. The system refines the calibration data through an optimization process that minimizes a reprojection errors function [26]. Reprojection error measures the difference between the observed 2D key-points in the images and the projected 2D locations of the 3D points calculated using the current calibration data. Pose quality assesses the plausibility of the calculated poses based on expected orientations and distances between key-points which have a defined range based on biological constraints (relative position of anatomical key-points to each other). The calibration parameters are then refined iteratively to reduce the reprojection error [26]. The system is robust to temporary occlusions and outliers by using temporal consistency checks.

The system outputs coordinates of the key-points in a 3D space for all objects present in the scene, and associates each keypoint to an object, differentiable by their track number consistent over frames, and a confidence metric (average 2D confidence from HRNET estimation over all 2D poses used to generate the 3D pose). The number of objects is determined by the number of unique key-points. To maintain tracking consistency in assigning key-points to the correct object across timestamps, the system employs a combination of spatial-temporal continuity and trajectory analysis. Once key-points are identified in each frame, the system tracks these points over time by assuming smooth and continuous motion, thereby associating key-points in one frame with their corresponding points in subsequent frames. This process creates trajectories for each keypoint, which are then used to distinguish between different objects based on their unique movement patterns. Additionally, the system incorporates a smooth motion error function during optimization, which penalizes non-uniform acceleration of key-points between frames, further ensuring spatio-temporal consistency. Fig. 1 exemplifies the 3D pose in two separate events by showing the vertical coordinate of key-points during STL for each track.

The pose estimator expresses coordinates in an approximation of the meter. It is important to note that while the scale of units expressed by the 3D key-points is consistent across locations, its exact resolution is unknown. This means that all values given in meters should be considered as $m \pm \mathbb{C}$ where $\mathbb{C}$ is an unknown constant. The implications of this limitation is that great caution should be exercised when comparing absolute values to other studies but that analysis of association and change rates are unaffected.

2.3. Video sequence selection

Initially, 979 videos showing a lying-to-standing bout and 1015 showing standing-to-lying were visually identified for development purposes [27] and reused for this study. We applied a simple event detector calculating the difference in average withers Z position (height) across 10 frames (0.3 s) between the start and end of the sequence. An absolute difference above 0.4 m was considered to be a posture transition, and the direction of change (downwards for STL and inversely) informed on the type. This is visible in Fig. 1 where the withers go from a height of about 1.7 m to 1 m.

After detecting events, 814 and 798 sequences were classified as lying to standing and standing to lying respectively. This corresponds to respective false negative rates of 16.9 % and 21.4 %. After visually inspecting the key-point series for each sequence, 5 and 26 sequences were noticed to have been misclassified as LTS and STL and subsequently removed, giving false positive rates of under 1 % and 3.2 %. The sequences contained the 30 to 35 s video recorded by 7 synchronized cameras and show cows transitioning between postures in a cubicle. Removal of false positives left 809 and 791 LTS and STL sequences respectively.

2.4. Signal processing of 3D pose time series

2.4.1. Filtering

A low-pass filter with a cut-off frequency of 10 Hz was applied to each key-point and its corresponding X, Y and Z coordinates' time series individually. This approach is based on recommendation by Hamäläinen et al. [28] and by Riaboff et al. [29] for noise removal on animal motion data (originally intended for accelerometer data). The filter was implemented in Python 3.9 using the function "butter" from the SciPy package [30].

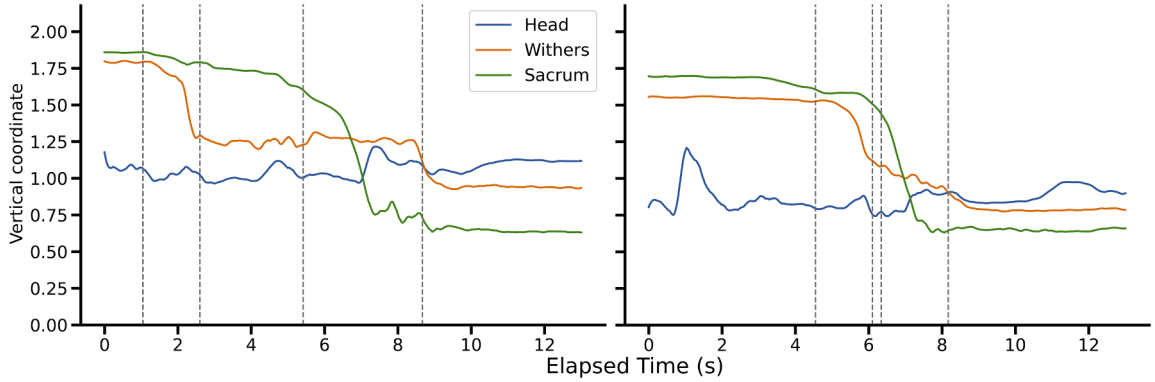

Fig. 1. Vertical coordinate of 3 key-points during two lying down motions, comparing slow with swift posture transitions. Dashed lines correspond to the detection of the initial leg bend, thoracic limbs on ground, sacrum descent and completion. On the right pane, the rapid sacrum descent initiates just before the front limbs touch the ground. These examples were cherry-picked for clarity.

2.4.2. Stitching discontinuous tracks

Object tracking could be interrupted by factors such as noise peaks or temporary occlusions, leading to instances where successive detections of the same animal were split between multiple tracks. To address this issue, we implemented a post-processing track-stitching algorithm that merges fragmented tracks corresponding to the same animal into a single continuous track, based on spatial continuity of the smoothened key-point coordinates. The track-stitching algorithm operates by first identifying all tracks within a given sequence and calculating the time and position at which each track ends. The algorithm then searches for subsequent tracks that begin within a temporal window of 1 s and spatial proximity of 0.3 (in the pose estimator's coordinate system, corresponding approximately to 30 cm). Candidate tracks that start shortly after the end of the previous track are evaluated based on their Euclidean distance in the 3D space, using the wither key-point's coordinate. The algorithm prioritizes merging tracks that are closest in space. Tracks are iteratively processed until no further stitching opportunities are detected. This method resulted in the inclusion of 305 LTS and 301 STL posture transitions sequences, representing 37.7 % and 38.1 % respectively of the total sequences used.

2.4.3. Interpolating missing poses

The tracking algorithm has a tolerance to punctual missing detections and stitched tracks had a gap up to 1 s. This resulted in instances where consecutive 3D poses were separated by more than the expected interval of 0.033 s. To ensure consistency, poses were interpolated for missing frames, thereby standardizing the time intervals between consecutive poses. First, gaps were identified based on the timestamp difference between consecutive poses, and the number of missing frames was calculated. We estimated missing poses using 3D cubic spline interpolation — a method Ren et al. [31] found to be highly faithful for interpolating missing positions in cow movement data—thereby achieving uniform temporal resolution across sequences and facilitating further calculations.

2.5. Indicators of posture transition quality

Indicators relevant to assessing the quality of the posture transition were retrieved from the literature and are listed in Table 1. This study focuses on the movement opportunities offered by the cubicles, and the occurrence of atypical motions. For this reason, inclusion criteria for indicators were (i) measurable during the posture transition movement and (ii) measurable through kinematic features at a specific phase of the posture transition. The start and end of the posture transition movements are described in Table 1. Atypical motions such as dog sitting and horse-like rising were initially selected but did not occur. The selected indicators, their definition and corresponding phase, as well as existing thresholds beyond which the motion is considered abnormal are gathered in Table 1.

Out of the selected indicators, lying down duration, hind quarters shifting, delayed rising, backwards crawling and head lunge space had quantified thresholds found in the literature. Side lunge was described as yes or no in the ethograms found in Brouwers et al. [15] and in Dirksen et al. [32].

Table 1
Selected indicators of posture transition comfort.

Indicator	Definition	Corresponding phases	Threshold for acceptable comfort
Rising			
Duration of rising motion	Start of the motion: the cow gathers its front limbs under the body causing a visible rise in the withers' position [27] End of the motion: the cow is fully up with all limbs extended [6]	Rising on breastbone, Standing	
Backwards crawling on carpal joints	When resting on carpal joints, the cow moves its front leg backwards before the lunge motion [12]	Rising on breastbone, lunge	None/0 m [12]
Delayed rising	The cow rests on its carpal joints before lunging.	Rising on breastbone, lunge	$<$ 10 s [12]
Head lunge distance	Euclidian distance projected in 2D above the bed, measured between the point of furthest extension of the head and the position of the withers just before the lunge (after possible backwards movements)	Lunge, head baseline location	$>$ 0.6 m beyond the end of the cubicle [22]
Side lunge	Maximum angle formed between the lines joining the poll to the neck and the neck to the t13 during the lunge [27].	Lunge	No side lunge [15,32]
Lying down			
Duration of lying-down motion	Start of the motion: one carpal joint is bent and lowered [11]. End of motion: the cow is fully lying down and the body is stable [12]	Initial leg bend, recumbent position	$<$ 6.3 s [11]
Hind quarter shifting	Duration between the moment both carpal joints touch the ground and the rapid descent of the sacrum.	Thoracic limbs touchdown, sacrum descent	$<$ 3 s [12]
Head displacement	Length of the horizontal vector between the head at start of the movement and its point of furthest forward displacement	Head maximum extension	0.59 m (mean maximum in open pen) [13]

2.6. Event detection during posture transition and indicator calculations

To measure the indicators of comfortable posture transition it was necessary to accurately detect the occurrence of specific phases during the motion using the key-points' displacement. These phases are listed in the third column of Table 1.

The main method here is change-point detection in the key-point coordinates, specifically the Y (perpendicular to the stall) and Z (vertical) coordinates of the withers. Change-point detection involves identifying indices in a time series where there is a shift in the series' statistical properties, such as mean or variance. In the case of the key-points 3D coordinates time series, change-points represent movements from one posture to another. The detection process involves segmenting the time series into distinct windows where the statistical properties are consistent within each segment but differ between segments. The change-points are the boundaries of these segments. Linearly penalized segmentation (Pelt) used here [33] optimizes the segmentation by balancing the number of change points against the fit to the data, using a penalty parameter to control the trade-off. The Pelt algorithm is implemented in the Python library Ruptures [34]. Parameters for change-point detection were optimized through a grid search testing the penalties of 3, 5 and 10 with any combination of the x and y coordinates of the withers or sacrum, and their movement velocity. For each combination, the mean absolute difference (MAD) was calculated between the annotated timestamp for that phase and the timestamp

corresponding to the nearest change-point. The variables and penalty creating a change point closest to the annotation are reported in the respective sub-section for each phase.

This method outputs several change-points in each sequence, corresponding to the different phases, as well as other events and also possibly noise. Thus it was necessary to select the right change point corresponding to the phase of interest amongst the various change-points detected.

The velocity of the withers and sacrum display specific patterns in between each phase as the cow moves parts of its body in succession. Thresholds in velocity peaks were used to constrain time windows for each phase and thus select the correct change-point. Rules and thresholds for change-point selection are described in Table 2 and in the subsections dealing with the detection of specific phase. It was not possible to detect all events in all sequences, and the final sample sizes used to calculate each indicator are found as labels on 3 and Fig. 5 respectively in the results section.

Fig. 1 Illustrates two STL sequences on which the timestamps detected for the phases have been marked by dashed vertical lines. On the left panel, the initial drop of the withers (orange curve), corresponding to the leg bend, was detected to have occurred at 9.6 s (first vertical dashed line). This is followed by readjustment movements of the hind quarters while the cow is standing on its thoracic limbs between the 11.8 s and 14.1 s timestamps. This characterised by a plateau of the withers height, as the cow rests on its anterior limbs during the posterior readjustment movements. On the example on the right, the motion is a lot swifter, with only a brief deceleration of the withers' descents, as both anterior limbs reach the ground at 15.2 s.

The methods to detect most phases are listed in Table 2. Other phases as well as kinematic indicators have a dedicated sub-section.

2.6.1. Backwards crawling

Before lunging, when forward space is perceived as insufficient the cow moves its front limbs backwards [12]. Identifying this movement enables to quantify the crawling distance but also enables the establishment of a consistent baseline position of the withers immediately prior to the head lunge, which is crucial for calculating the displacement of the head during the lunge. Backwards crawling was defined as the total backwards displacement of the withers key-point's coordinate along the x axis, between the start of the rising motion and the head lunge.

Table 2
Posture transition phases and methods for detection.

Posture transition phase	Penalty	Variables for change-point detection	Threshold for selecting a cv-hange-point
Rising (LTS)			
Start of rising motion	10	Withers Y, Withers Z	First change point where the median Z withers in the following 1 s window > median Z withers in the initial 1 s of the sequence
Head lunge	Maximum Head X coordinate		
Standing	5	Withers velocity	First change point after the last velocity peak of 0.18 (normalized units)
Lying down (STL)			
Initial leg bend	10	Withers vertical velocity	Last change point before the first peak in withers velocity above 0.2 (normalized units)
Thoracic limbs touchdown	3	Withers Z	First change-point immediately after the first peak above 0.2
Sacrum descent	Random forest		
Recumbent position	10	Withers Y, Withers Z	Last change point where the median Z withers in the following 1 s window < median Z withers in the final 1 s of the sequence

2.6.2. Head displacement and angle

For the analysis of head lunge, sequences were only used if the head key-point maintained a confidence level above 0.77 during lunge. The confidence threshold was decided by plotting the distribution of confidence values of the head around the predicted lunge timestamp, and visually identifying an elbow in the plot.

The withers baseline position was defined as the X coordinate of the withers after backwards crawling, also corresponding to the minimum X coordinate between start of the rising motion and lunge when crawling was not detected to have occurred. Lunge distance was defined as the distance on the x axis between the head at lunge and the withers baseline location, to which was subtracted the distance between the head and the withers at lunge. The rationale behind this calculation was to determine how far forward the head was able to lunge, not compared to the cubicle, but to the initial placement of the cow before lunging.

Head lunge angle was calculated as the 2D projected angle over the horizontal plane, formed by the line of the back (joining the withers to the sacrum) and the neck (joining the withers to head keypoint) at the moment of furthest extension. An angle of 180° represents straight lunge, where the head is exactly aligned with the back. A lower angle represents a sideways neck, independent of lunge side. (Fig. 2)

For the head displacement when lying down, the maximum filtered coordinate of the head on the X axis (parallel to the stalls) was subtracted to the head's position on the X axis at the time of initial leg bend.

2.6.3. Thoracic limb touchdown

This refers to the earliest point at which both anterior limbs are folded and the cow touches the bed with both carpal joints. The withers' coordinate was normalized and their vertical velocity was computed. Change-point detection with a penalty of 3 was applied to the withers Z coordinate series. Peaks in the wither's vertical displacement above 0.2 normalized distance units per second were detected, with a minimum distance between peaks of 40 points or 1.33 s. We selected the first change-point following the peak first.

2.6.7. Sacrum descent

The change-point method failed to produce detections corresponding to the sacrum descent timestamp. Instead, the following methods were tried: recurrent neural network with dropout and one of each 1 dimension convolutional, bi-directional long-short-term-memory and dense layers, against a random forest with 50 estimators predicting the index of the event. The RNN produced a MAE on unseen data between detections and annotations of 0.81 s at the stabilisation of the loss term after 12 epochs while the random forest produced a MAE of 0.41 s and was thus chosen. Since the sequences were of varying length and usually centred on the posture transition, and to avoid overfitting the model to a specific location in the sequence, the key-point series were randomly padded before training the models. Padding was added at the beginning and end of each series, for a total length of 1147 (arbitrary value above the length of the longest series) according to the following equations:

L_{pad_s} is the total padding length for sequence s: $L_{pad_s} = 1100 - L_s$ with L_s being the length of sequence S.

L_{start_s} is the padding length at the start of sequence s: $L_{start_s} \sim Uniform(0,\ L_{pad_s})$

L_{end_s} is the padding length at the end: $L_{end_s} = L_{pad_s} - L_{start_s}$. The padding values are calculated as follows:

$$P_{pos,\ k,\ x} = coord_{pos,k,x} \otimes I_{L_{pos}*1} + N \quad (1)$$

where P is the matrix of padding values of size $6 * L_{pos}$ with pos taking values $start$ or end, $coord$ being the first or last value in the series for coordinate $x = X$ or Z and key-point $k =$ withers or sacrum. $N \sim Uniform(0,\ 0.05)$ is a vector of random noise. Considering S, the original sequence of key-point positions, the padded sequence used as input in

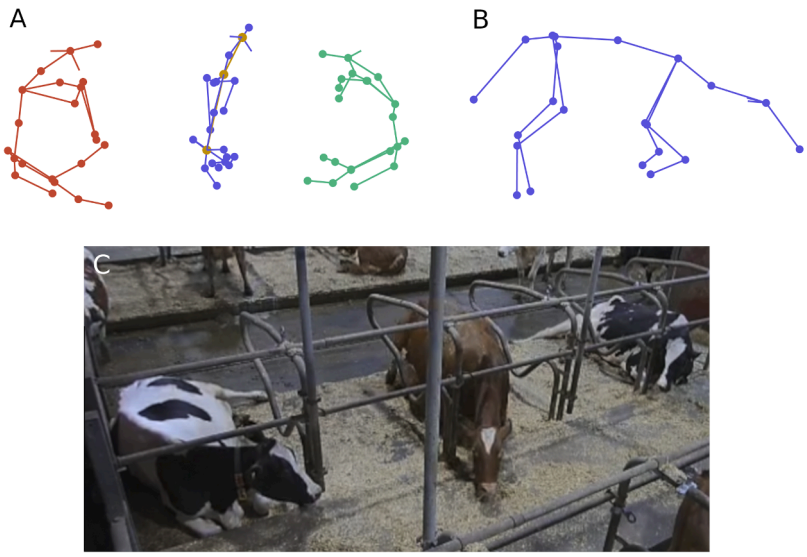

Fig. 2. 3D pose of cows with one cow rising (blue pose) taken at furthest head extension (lunge). Head lunge angle is defined as the angle between the segments in yellow on pane A, joining the head, withers and sacrum (highlighted). A: top down view of all 3D poses in the row of cubicles. B: side view 3D pose of the cow rising. C: corresponding frame.

the random forest is:

$$\begin{bmatrix} P_{start} \\ S \\ P_{end} \end{bmatrix}$$

2.7. Validation

2.7.1. Agreement between observers and with event detection

To validate the accuracy of the detection of the various phases, video sequences showing posture transitions by a single cow were annotated by 3 observers. The observers annotated the timestamps for each event listed in column 3 of Table 1. Observers first trained on 10 sequences for each posture transition and agreed on the timestamps to annotate. Then, each observer was provided with a total of 100 video sequences for each posture transition, which were randomly assigned, shuffled and blinded. The 100 sequences contained 55 videos which were common to all observers. This overlap was to score inter-observer agreement. The 100 videos also contained 30 sequences which were unique to each observer. Among the resulting 85, 15 were randomly resampled to assess intra-observer agreement. For each sequence to be annotated, the material provided to the observers contained the synchronized video from all 7 cameras. Observers were free to choose the camera offering the best view of the cow performing the posture transition.

Agreement was measured as MAD between annotated and detected timestamps. $MAD(i,m) = \frac{1}{300}\sum_{s=1}^{300}\left|\Delta_{s,(o,m)}\right|$ where $\Delta_{s,(o,m)} = \left|t_{s,i} - t_{s,m}\right|$ with m being the automated detection and $t_{s,i}$ the time stamp of the s:th sequence by o:th observer.

2.7.2. Agreement depending on interruptions in the poses

Sequences contained 637 to 1013 consecutive poses, including sequences stitched from spatio-temporally continuous tracks. We ran a regression to analyse the effect of the presence of a stitch in a ± 1.7 s window around the annotation, as well as the duration of interpolated poses on the agreement between annotations and detections. The model is described as follows:

$$T_{o_e} = \beta_1 + \beta_2 M + \beta_3 S + \beta_4 I + 1|sequence + \varepsilon \quad (2)$$

where T is the observed timestamp, either annotated or detected. e is the event (taking values of all 7 events in both posture transitions). M is the observer type indicating whether the timestamp was annotated by a human or detected by the model. S is a dichotomous variable representing the presence of a track-stitch in the 3D pose sequence. It always takes the value of 0 in the case of human annotation (because stitches in the 3D pose have no meaningful effect on human annotations performed on the video), and 1 or 0 in the case of model detections, depending on the presence of a stitch in the ±1.7 s window around the mean human annotation. The value of 1.7 s corresponds to the 95th percentile of differences between human and machine. Similarly, I is the interpolated duration in case of detections and 0 in the case of annotations. Finally, $1|sequence$ represents a random intercept for the sequence number, as the predicted timestamp in each sequence has no tangible meaning and is relative to the start of the video but should theoretically be equal for all annotations in the same sequence. We report the value and the significance of β_2, β_3 and β_4. β_2 represents the difference in predicted event timestamp if the observation was done by the model compared to a human, β_3 the change in predicted timestamp if the observation was done by the model and a stitch was present in the ±1.7 s window and β_4 the change in predicted timestamp for 1 s of interpolated poses in the window. Significance is accepted at a risk of $\alpha = 0.05$.

2.8. Exclusion criteria

Sequences were first included if a posture transition was detected from the key-point data. This produced 809 sequences in which the occurrence of a LTS posture transition was visually identified, and 791 STL. Regarding annotations, 145 sequences of each posture transition were originally annotated. 4 annotated STL sequences were discarded as well as 4 LTS sequences because of data quality issues.

After the events of interest were detected using the methods described above for the entirety of the sequences, including all sequences which had not been annotated, the validity of the detection was visually assessed using the vertical displacement graphs, of which Fig. 1 shows an example for two different sequences. The time-series of the key points' vertical coordinate were plotted for all sequences, and the detected timestamps were added to the plots. Sequences were excluded based on visual assessment if any of the detected timestamps did not match the kinematic pattern corresponding to the event. 84 LTS and 87 STL sequences were excluded, the number of events that were inaccurately detected is listed in Table 3.

Table 3
Count and frequency of detection errors per event. Note that the total errors amount to more than the total, as several events could be off in the same sequence.

Event	Errors	Frequency
Rising (LTS)		
Rise on breastbone	22	2.7 %
Lunge	34	4.2 %
Standing	37	4.6 %
Any	84	10.4 %
Lying down (STL)		
Initial leg bend	17	2.2 %
Thoracic limbs touchdown	29	3.7 %
Sacrum descent	36	4.6 %
Recumbent position	13	1.6 %
Any	87	11.0 %

2.9. Statistical analysis of indicator scores

To explore the association between indicators, Spearman's correlation was calculated between indicators in the same posture transition sequence. A principal component analysis (PCA) was conducted to identify more complex correlations between indicators in LTS transitions using PCA function from SciKit-Learn [35].

3. Results

The purpose of this study was to evaluate the accuracy in the detection of the successive stages in the posture transitions, to detect the occurrence of indicators exceeding thresholds for comfortable posture transition and to explore possible indicator association.

3.1. Comfort indicators exceeding thresholds

In the stalls used for this study, and regarding duration, we found that 2.8 % of LTS posture transitions exceeded the threshold for indicator 'Rising delay'. If we use the 5 s threshold used in Fråga Kon, instead of 10 s found by Zambelis et al. [12], 30.2 % of LTS bouts would exceed the threshold. Crawling backwards occurred in 59.2 % of LTS transitions. 28.9 % of STL exceeded the threshold for total duration and 8.3 % for shifting duration. Altogether, 59.9 % of LTS and 29.1 % of STL exceeded thresholds for at least one indicator.

Table 4
Mean absolute difference (in seconds, ± standard deviation) in annotated or detected timestamps for each pair of observers and with the automated detection.

Feature	Observer pair			
	Obs 1 - 2	Obs 1 - 3	Obs 2 - 3	Observers – machine
Rising (LTS)				
Rise on breastbone	1.1 ± 1.4	1.8 ± 1.6	1.0 ± 1.3	0.9 ± 1.1
Head lunge	0.2 ± 0.3	0.2 ± 0.4	0.2 ± 0.4	0.3 ± 0.6
Standing	0.5 ± 1.1	0.6 ± 1.1	0.4 ± 0.4	0.7 ± 0.9
Lying down (STL)				
Leg bend descent	0.3 ± 0.2	0.2 ± 0.2	0.2 ± 0.2	0.4 ± 0.7
thoracic limbs touchdown	0.2 ± 0.1	0.2 ± 0.1	0.2 ± 0.1	0.4 ± 0.6
Sacrum descent	0.4 ± 0.4	0.4 ± 0.4	0.3 ± 0.4	0.4 ± 0.5
Recumbent position	0.8 ± 0.4	0.5 ± 0.5	0.5 ± 0.6	0.4 ± 0.7

3.2. Agreement on phase detection and robustness to interrupted poses

The results in Table 4 show agreement under half a second for most events. The first phase of the rising movement showed the most disagreement between observers. (Table 5)

When missing positions were interpolated, the average interpolated duration was 0.5 $s \pm 0.5$ (μ±σ) or 31 % of frames in the window around the event for LTS and 0.7 ± 0.7 or 43 % of frames for STL. For both rising and lying down transitions, interpolating poses on missing frames did not have a significant effect on the timestamp prediction by the model. Only for the rising on breastbone and the thoracic limbs touchdown phases did the presence of a stitch have a significant effect on the difference between annotated and detected timestamps (at $\alpha = 0.05$). The observed timestamp being detected by the model rather than a human observer was only significant for the thoracic limbs touchdown.

3.3. Distribution and association of posture transition comfort indicators

The analysis of association between indicators was aimed at understanding whether there existed a combination of indicators which by themselves offer a summary of the posture transition quality, or rather if indicators showed no association and that there was thus no relation between the qualities of the different phases. Both posture transitions were analysed separately.

3.3.1. Lying to standing

Rising duration had a median of 8.3s±2.8 (median ± Standard deviation) and a skewness of 1.4. Total duration does not have a threshold on Fig. 3 since no recommendations were found. For rising delay, it was 4.0s±2.4 with a skewness of 1.4. Crawling distance had a median of 0.1 ± 0.1 and a skewness of 1.1. Lunge distance showed an important range from 0.3 to 1.5. Its median was 0.66±0.33 and its skewness 0.44. Lunge angle had a median of 159.7° ± 11 and its distribution was skewed to the left (skewness −0.6).

Spearman's pairwise correlations, shown as labels on Fig. 3 revealed a set of moderately to strongly correlated variables ($p < 0.001$): duration, crawling distance and rising delay. Lunge angle and distance had a negligible yet significant correlation ($p = 0.005$), the significance driven by the high sample size ($n = 548$). (Fig. 4, Fig. 5)

The principal component analysis aimed at exploring whether the indicators could be combined into subsets that better explain the movement patterns. The first 4 components were retained, explaining 98 % of the variance in the dataset.

The first component (PC1) explains 45 % of variance. Variables with the highest loading on PC1 were delay, crawling and duration. The second component (PC2) explains 23 % of the variance and is loaded by head lunge distance and angle.

Table 5
Coefficients for the effect of the processing method and event detection on the predicted timestamp based on Eq. (2). Significant coefficients are bolded.

Feature	Coefficient for the effect on predicted timestamp (seconds) (n sequences with processing method)			ICC
	Presence of stitch	Duration of interpolation	Model detection	
Rising (LTS)				
Rise on breastbone	**−1.4** (7)	0.0 (27)	−0.1	0.83
Head lunge	−0.4 (10)	0.1 (72)	−0.0	0.87
Standing	0.3 (14)	0.4 (32)	−0.1	0.78
Lying down (STL)				
Leg bend descent	−0.0 (9)	−0.3 (38)	−0.1	0.91
thoracic limbs touchdown	**−0.5** (18)	0.1 (91)	**−0.4**	0.95
Sacrum descent	−0.1 (29)	0.0 (14)	−0.0	0.94
Recumbent position	0.2 (7)	0.3 (30)	−0.0	0.83

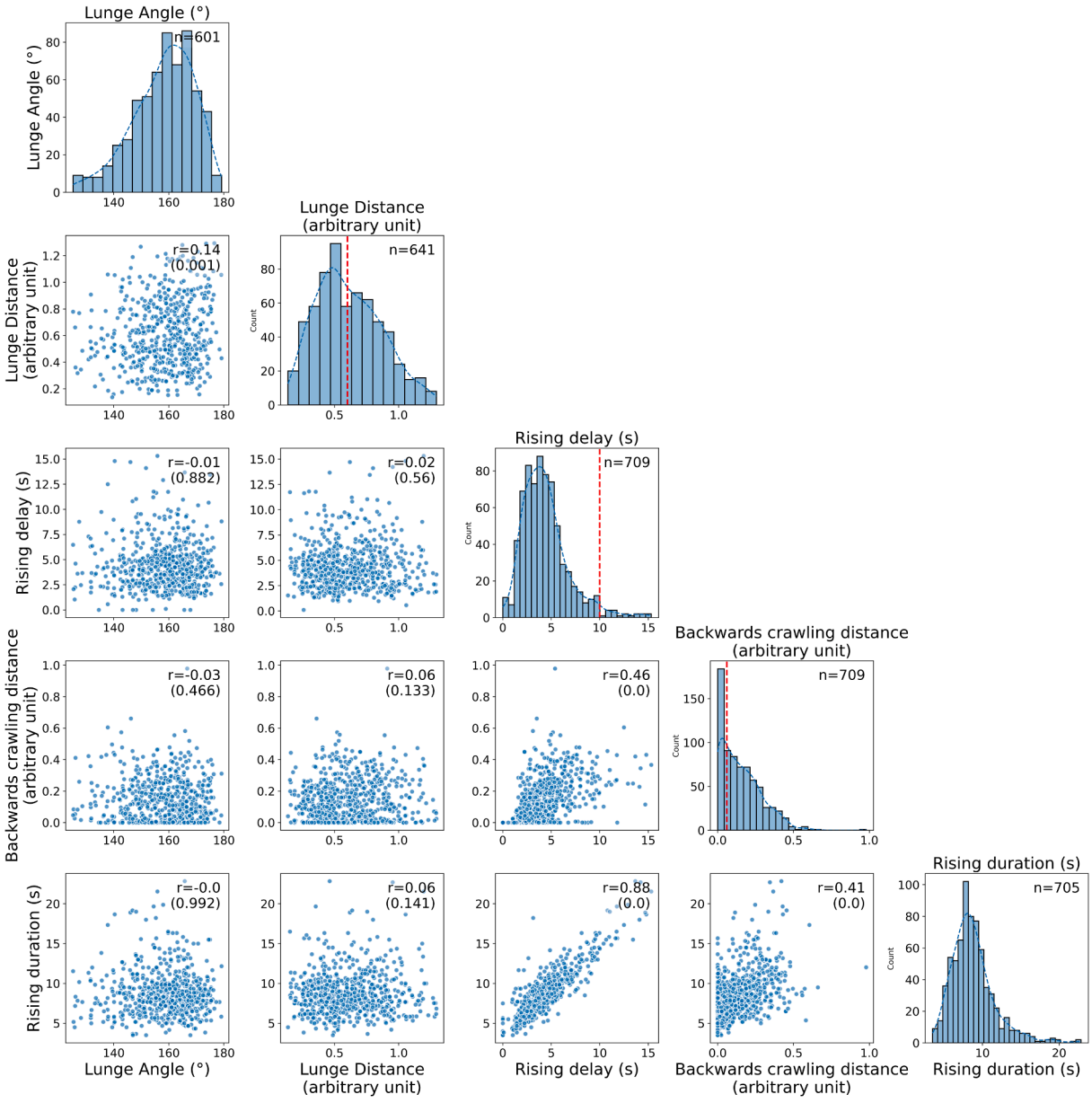

Fig. 3. Distribution with kernel density estimation and pairwise scatterplots of lying to standing posture transition indicators. Cut-offs for comfort assessment are indicated by a dashed red line on the histograms when found in the literature. The sample size for each indicator is reported with the histograms and the correlation (p-value) on the scatterplots.

Components 3 and 4 explained 17 and 13 % of variance respectively. Component 3 had lunge angle and distance load with opposing signs. Component 4 showed opposed loading signs between duration and crawling distance.

3.3.2. *Standing to lying*

The Spearman correlation between shifting duration and lying down duration is 0.66 ($p < 0.001$). Lying down duration had a median of 5.6 ± 1.7 and a skewness of 2.2 while shifting duration had a median of 1.4 ± 1.2 and skewness of 2.4. The distribution of shifting duration is unbalanced, with a high frequency at 0 because of bouts not displaying a window for hind quarter shifting.

4. Discussion

The study comprises several final and intermediate results, which all have implications for dairy cow comfort monitoring in free stalls using pose estimation in 3D This discussion will first offer a summary of key findings regarding both validation of the method and indicator scores, it will then compare them with earlier research and discuss limitations and implications for future cattle welfare monitoring.

4.1. *Validation and agreement with human observation*

The results confirmed a high agreement between human and algorithmic detection of posture transition phases. The agreement between human and machine in detecting the timestamp of specific events has two implications. The first one is that we can use the system to measure the duration of the successive phases of the posture transition, which is a comfort indicator. The second implication is that the 3D capture system properly captures the kinematics of events of interest since what is seen on the video matches change points in the 3D coordinates. We note that the development was done with a single cubicle design and that the algorithm may not perform equally well in other systems. Supervised

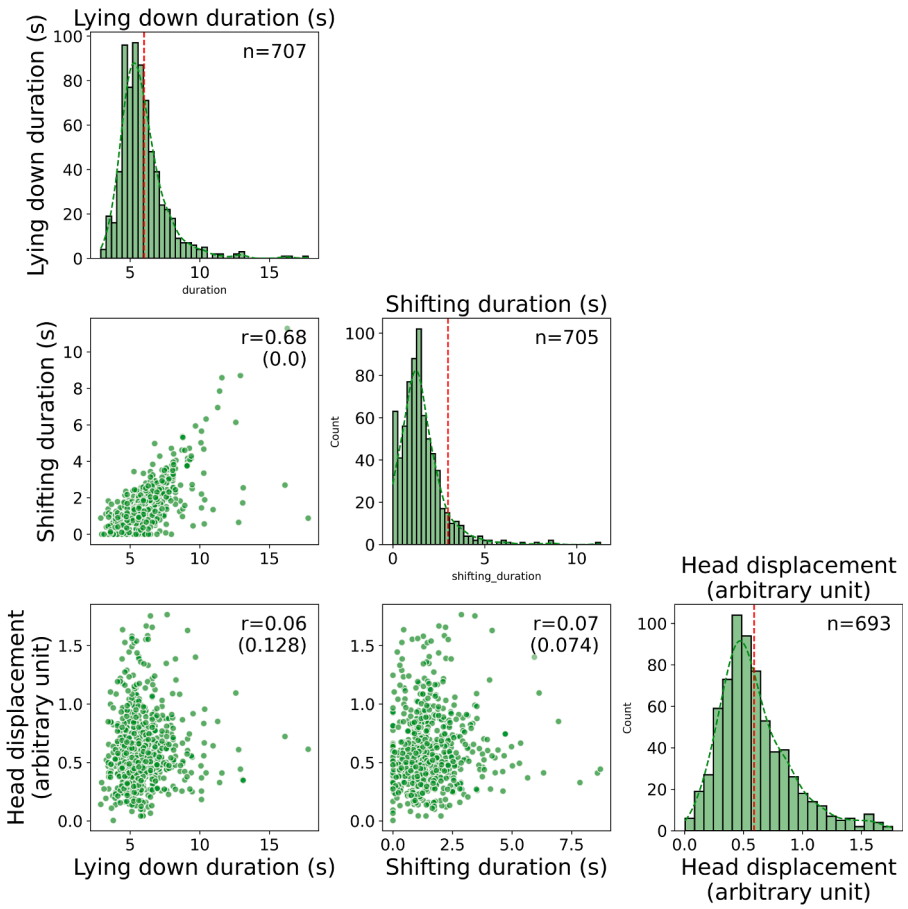

Fig. 4. PCA biplot for lying to standing indicators showing variable loadings and individual scores on 4 components.

learning methods for event detection using diverse sequences can likely address this limitation. The failure rate of up to 11 % does mean that human supervision is required before making meaningful conclusions.

4.2. Comparison of the results with previous studies

Most STL sequences (71 %) were within the accepted duration, however backwards crawling during LTS was highly prevalent. This prevalence comes in stark contrast to results by Brouwers et al. [36] who found a probability of backwards crawling no higher than 5 % in different cubicles. These differences are likely imputable to different stall designs. Zambelis et al. [12] did not find backwards crawling to be associated with characteristics of the cow, nor with adverse welfare outcomes. We still found the indicator be included in the Fråga Kon manual. Combined with the fact that it is rarely observed in unrestricted environments [6], lead us to advocate for its inclusion when evaluating cubicle designs.

Delayed rising; or a pause before the swift head lunge movement, above the suggested threshold had a low prevalence in our study (2.8 %), compared with the 19.5 % reported by Zambelis et al. [12], hinting again at the fact that indicator distributions vary greatly with stall design and thus that the results presented here should not be extrapolated to other farm settings.

The range of forward head displacement shows that even if forward lunge space is offered, cows use this space very differently. We observed on the video that some cows had slow and hesitant movements, with the head not extending beyond the head rail, while others would lunge far forward, potentially explaining the measured variability. Thresholds exist for lunge room, for example 0.9m according to Cook [3]. The 3D coordinates in the system used here however were not precisely expressed in meters. Although the system approximates the meter by design in the calibration phase, caution is warranted when comparing displacement measurements to previous results.

Rising duration is dependent on the identification of the start of the rising motion, which is the phase with the highest ambiguity to observers (over 1 s average difference). Rising duration was positively associated with cow width in the study by Zambelis et al. [12], while delayed rising was not. Delayed rising was a binary indicator in the latter study [12]. Larger cows were predicted to lunge further in an earlier study [37]. A possible explanation for both these results is that larger cows are more hesitant throughout the bout but not specifically before lunge. In the Fråga Kon framework, the threshold for delayed rising was 5 s instead of 10, which would lead to a different observed prevalence.

4.3. Assessing comfort with a combination of indicators and 3D pose

In the Welfare Quality framework, posture transitions are assessed using two indicators; duration and collisions [11]. In their “Flowchart for Evaluating Free Stalls”, Nordlund [38] assesses posture transitions through lunge and “bob” spaces, and rising room (measured as the absence of collisions). The manual for Fråga Kon uses the duration of the pause on the front limbs as main indicator. It exemplifies abnormal rising with backwards crawling, dog sitting and difficulty to rise (assessors have also stated looking at side lunge), and gives the expert assessor the discretion to judge, looking at a more complete picture of the cow. Taken separately, indicators provide a simplified view, which is practical for on-farm applications but may not capture the full complexity of the posture transition process.

According to the PCA, there are several uncorrelated patterns of rising motions. PC1 is interpreted as corresponding to hesitation,

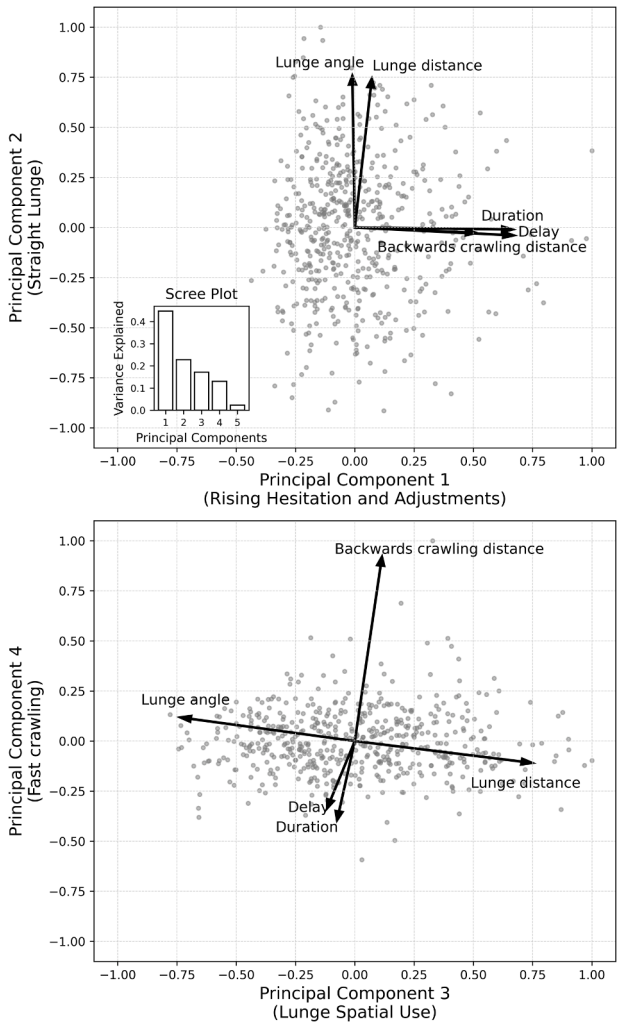

Fig. 5. Distribution with kernel density estimation and scatterplot of standing to lying posture transition indicators. Cut-off for shifting duration is indicated by a dashed red line on the lower histogram. The sample sizes for both indicators are reported with the histograms and the correlation (p-value) on the scatterplot.

creating pauses in the rising motion. This is because the variables loading the highest on PC1 are delay, crawling distance and total duration. These variables are correlated, which is sensible since the further a cow will crawl, the more time it needs to do so, which increases delay and total duration directly. PC2 represents straight lunge, which is a desirable pattern. Lunge distance and angle had a low correlation, but they loaded similarly on PC2, suggesting that they measure distinct but complementary aspects of lunge behaviour. There is seemingly an upper diagonal bound on the scatterplot for these two variables (Fig. 3) which would indicate that angled lunges rarely are associated with longer distance. Components 3 and 4 seem to show exceptions from the most common motion patterns; component 3 had lunge angle and distance load with opposing signs, representing both lateral and longitudinal spatial use while bouts scoring high on PC 4 would represent cows crawling an important distance but quickly.

Principal components being uncorrelated implies that crawling (PC1) is not associated with straight lunge (PC2), contrary to what we had previously hypothesized (the rationale being that crawling backwards offered more forward space to then lunge straight). We know that the stall design in the study farm promotes backwards crawling, which tends to increase delayed rising through readjustments as is reflected in PC1. Loadings on PC4 however show an opposite pattern where cows do crawl but swiftly. Taken together, PC1 and PC4 imply that duration is not systematically an indication of crawling. The first component suggests that the proxy indicator found in Welfare Quality or Fråga Kon are sound summarisation of the parameters explaining the most variability, but the other components suggest that there are additional dimensions to the quality of posture transitions which we should not summarise into a single indicator.

4.4. *Defining thresholds based on existing variability and quantitative measurements*

The distribution of indicator values presented in the results highlights that the range of posture transition movements, and the duration of the different phases exist on a continuum. This comes in stark contrast with the rigid thresholds found in the literature which may not be adapted to assessment using sensor data, of which lunge angle is a clear example. In a similar development, Brouwers et al. [15] found moderate accuracy (60 %) in detecting the occurrence of side lunge using accelerometer data. While the class for side lunge was yes or no, there seems to exist a continuum of lunge angles as shown on the first density plot of Fig. 3. It is worth exploring if misclassifications happen more consistently when the head lunge is at a slight angle. This would mean that the challenge in classifying side lunge in the latter study is not a shortcoming in the algorithm but rather a limitation in the ethogram used in annotations which is not adapted to continuous data [15]. This might lead to misalignments between the sensor output and the annotation, especially in the range of neck angles that represent the borderline between normal and abnormal lunge angle. Bewley et al. [39] describe side lunge as that performed in cubicles designed specifically to allow for cows to lunge their head side, instead of forward (because the cow could be impeded by a wall or another cow). We saw accordingly, in studies assessing posture transitions, that side lunge was a yes/no indicator [12,15]. In the study presented here, the cubicles were designed for forward lunge. However, we did both observe and record bouts in which the neck was at an angle compared to the head. It is important to define whether this form of angled forward lunge classifies as side lunge, if it is another form of abnormal lunge, or if rather it should not be considered abnormal but an individual preference. Anecdotally expert assessors judged some of the lunges in our study as being sideways, yet we found no apparent cut-off in the distribution of lunge angles. This hints to the fact that side lunge is more complex than forward versus sideways, but that there also may not be a universal threshold for what angle constitutes side lunge. This trend towards not observing clear cut-offs from the distribution is visible in all the indicators measured here. We propose that assessment of posture transitions using sensor data should not be done against a rigid threshold. This technology paired with individual recognition could quantify the variability within the herd and individuals, help understand individual motion patterns and tailor the benchmarks to each cow.

4.5. *Limitations and necessary improvements for practical implementation*

In our previous study, validating a data processing method to detect the start of the rising motion, using the same key-points, we had excluded sequences for which the rising motion was split into several tracks [27]. In real world settings, data generation mechanisms will inevitably produce gaps. In order to move towards implementing such tools in practice, it was important to test whether interrupted sequences could still provide an accurate detection of the posture transition phases. The results were encouraging and showed that stitching tracks and interpolating poses had little effect on the accuracy of the event detection.

Improvements should be made in the system to obtain coordinates in meters, which would allow comparing lunge room with earlier studies [6,13,40]. This would also help provide recommendations regarding

cubicle dimensions based on spatial use [2].

Challenges remain for practical application, namely dealing with inaccuracies in event detection and the high false negative rate. The current detection method was a rule-based approach, which relies on the high interpretability of 3D pose estimation, reflecting the actual movement amplitude and location of the anatomical features. This high interpretability can reduces the amount of annotated data needed for event detection and can be relied upon to verify the validity of the detections by setting numerical constraints based on the assumed relative location of the key-points, to each other and to their previous location. Once we identify the kinematic pattern of a phase, we can split longer key-point time series into windows and find matching patterns.

For the head lunge space threshold, we used an average forward displacement of 0.6 m reported by [6]. It is consistent with the findings of [13] who reported a mean maximum displacement of 0.59 m when lying down. This however remains an average and quantifying the variability within the herd is instrumental in designing stall elements which can accommodate all cows.

More posture transition indicators exist than were used in this study. A detailed list can be found in Zambelis et al., [12]. This study was, limited to kinematic indicators.

5. Conclusion

This study showed that 3D fusion of pose estimation is a possible sensor technology to complement posture transition assessment with kinematic measurements. It shows good accuracy on detecting events, with disagreements with human-made visual observations being under 0.5 s for most phases and 0.9 s at most. Human oversight is needed for final evaluation since up to 11 % of sequences had at least one incorrect detection.

Measuring posture transition indicators showed that over half of rising events and under a third of lying down events were considered abnormal. Backwards crawling before rising was particularly prevalent in the farm and cubicles studied.

Analysing the association of indicators with a PCA showed that the dimensions of lunge, hesitation and spatial use were uncorrelated. Backwards crawling, delay, and head lunge should be assessed through specific indicators to cover these distinct dimensions separately. In practice, this is challenging to perform visually, and pose estimation offers a method to increase the information available to assessors.

Notes

The study presented here was approved by the ethical committee Uppsala djurförsöksetiska nämnd under approval 5.8.18–13,069/2021.

The authors thank the Swedish Research Council (Formas) for funding this research (grant 2021–02,254), the personnel of the Swedish Dairy Research Center at Lövsta for their help, and Sony Sweden for the extensive collaboration.

Sony Sweden provided the technology to generate the 3D pose. Conceptualization, study design, statistical analysis and presentation of the results were decided by researchers at the Swedish University of Agricultural Sciences. Sony Sweden contributed in drafting the methods section regarding key-point acquisition in 3 dimensions, and in revising the final manuscript.

Generative artificial intelligence (AI) was used to rephrase paragraphs and improve readability as well as to generate code for the analyses.

Ethical statement

This manuscript involves non-invasive research on 183 animals (*Bos taurus*). The authors declare that all procedures in the submitted work were conducted in accordance with national regulations regarding the use of purpose-bred research animals. The research was approved by the ethical committee Uppsala djurförsöksetiska nämnd under approval 5.8.18-13069/2021.

CRediT authorship contribution statement

Adrien Kroese: Writing – review & editing, Writing – original draft, Visualization, Validation, Methodology, Investigation, Formal analysis, Conceptualization. **Niclas Högberg:** Writing – review & editing, Validation, Supervision, Resources, Project administration, Methodology, Investigation, Funding acquisition, Conceptualization. **Elena Diaz Vicuna:** Writing – review & editing, Methodology, Investigation. **David Berthet:** Software, Resources, Data curation, Conceptualization. **Nils Fall:** Writing – review & editing, Supervision, Project administration, Funding acquisition. **Moudud Alam:** Writing – review & editing, Visualization, Validation, Supervision, Methodology, Formal analysis. **Lena-Mari Tamminen:** Writing – review & editing, Visualization, Supervision, Methodology, Funding acquisition, Formal analysis.

Declaration of competing interest

The authors declare the following financial interests/personal relationships which may be considered as potential competing interests:

Sony provided the technology to generate the 3D pose. Conceptualization, study design, statistical analysis and presentation of the results were decided by researchers at the Swedish University of Agricultural Sciences. Sony contributed to drafting the methods section regarding key-point acquisition in 3 dimensions, and in revising the final manuscript. This study was not performed with the intent of supporting a commercial or competitive claim.

Data availability

The authors do not have permission to share data.

References

[1] J. St. John, J. Rushen, S. Adam, E. Vasseur, Making tiestalls more comfortable: I. Adjusting tie-rail height and forward position to improve dairy cows' ability to rise and lie down, J. Dairy Sci. 104 (3) (2021) 3304–3315, https://doi.org/10.3168/JDS.2019-17665.

[2] N.B. Cook, Free-stall design for maximum cow comfort, WCDS Adv. Dairy Technol. 21 (21) (2009) 255–268. https://acrre.ualberta.ca/wp-content/uploads/sites/57/wcds_archive/Archive/2009/Manuscripts/FreeStallDesign.pdf.

[3] N.B. Cook, Optimizing resting behavior in lactating dairy cows through freestall design, Vet. Clin. North Am.: Food Animal Practice 35 (1) (2019) 93–109, https://doi.org/10.1016/J.CVFA.2018.10.005.

[4] S.P. Brouwers, M. Simmler, M.F. Scriba, P. Savary, Cubicle design and dairy cow rising and lying down behaviours in free-stalls with insufficient lunge space, Animal (2024) 101314, https://doi.org/10.1016/J.ANIMAL.2024.101314.

[5] S.S. Nielsen, J. Alvarez, D.J. Bicout, P. Calistri, E. Canali, J.A. Drewe, B. Garin-Bastuji, J.L.G. Rojas, C.G. Schmidt, M. Herskin, V. Michel, M.Á.M. Chueca, B. Padalino, H.C. Roberts, H. Spoolder, K. Stahl, A. Velarde, A. Viltrop, A.D.B. des Roches, C. Winckler, Welfare of dairy cows, EFSA J. 21 (5) (2023), https://doi.org/10.2903/j.efsa.2023.7993.

[6] L. Lidfors, The use of getting up and lying down movements in the evaluation of dairy cattle environments, Vet. Res. Commun. 13 (4) (1989) 307–324, https://doi.org/10.1007/BF00420838.

[7] C.B. Tucker, D.M. Weary, Stall design: enhancing cow comfort, Adv. Dairy Technol. 13 (2011) 155–167. https://www.researchgate.net/publication/255658372.

[8] M.B. Jensen, L.J. Pedersen, L. Munksgaard, The effect of reward duration on demand functions for rest in dairy heifers and lying requirements as measured by demand functions, Appl. Anim. Behav. Sci. 90 (3–4) (2005) 207–217, https://doi.org/10.1016/J.APPLANIM.2004.08.006.

[9] D.B. Haley, J. Rushen, A.M. de Passillé, Behavioural indicators of cow comfort: activity and resting behaviour of dairy cows in two types of housing, Can. J. Anim. Sci. 80 (2) (2000) 257–263, https://doi.org/10.4141/A99-084.

[10] C. Tucker, D. Weary, D. Fraser, Free-stall dimensions: effects on preference and stall usage, J. Dairy Sci. 87 (5) (2004) 1208–1216, https://doi.org/10.3168/jds.S0022-0302(04)73271-3.

[11] H. Blokhuis, M. Miele, I. Veissier, B. Jones, in: H. Blokhuis, M. Miele, I. Veissier, B. Jones (Eds.), Improving Farm Animal Welfare, Brill | Wageningen Academic, 2013, https://doi.org/10.3920/978-90-8686-770-7.

[12] A. Zambelis, M. Gagnon-Barbin, J.S. John, E. Vasseur, Development of scoring systems for abnormal rising and lying down by dairy cattle, and their relationship

with other welfare outcome measures, Appl. Anim. Behav. Sci. 220 (2019), https://doi.org/10.1016/j.applanim.2019.104858.
[13] A. Ceballos, D. Sanderson, J. Rushen, D.M. Weary, Improving stall design: use of 3-D kinematics to measure space use by dairy cows when lying down, J. Dairy Sci. 87 (7) (2004) 2042–2050, https://doi.org/10.3168/JDS.S0022-0302(04)70022-3.
[14] F.J. Lawin, A. Byström, C. Roepstorff, M. Rhodin, M. Almlöf, M. Silva, P. H. Andersen, H. Kjellström, E. Hernlund, Is markerless more or less? Comparing a smartphone computer vision method for equine lameness assessment to multi-camera motion capture, Animals 13 (3) (2023) 390, https://doi.org/10.3390/ani13030390.
[15] S.P. Brouwers, M. Simmler, P. Savary, M.F. Scriba, Towards a novel method for detecting atypical lying down and standing up behaviors in dairy cows using accelerometers and machine learning, Smart Agric. Technol. 4 (2023) 100199, https://doi.org/10.1016/J.ATECH.2023.100199.
[16] C.-H. Lee, T. Mendoza, C.-H. Huang, T.-L. Sun, Vision-based postural balance assessment of sit-to-stand transitions performed by younger and older adults, Gait Posture 117 (2025) 245–253, https://doi.org/10.1016/j.gaitpost.2025.01.001.
[17] X. Kang, X.D. Zhang, G. Liu, A review: development of computer vision-based lameness detection for dairy cows and discussion of the practical applications, Sensors 21 (3) (2021) 753, https://doi.org/10.3390/s21030753.
[18] A. Nejati, A. Bradtmueller, E. Shepley, E. Vasseur, Technology applications in bovine gait analysis: a scoping review, PLoS ONE 18 (1) (2023), https://doi.org/10.1371/journal.pone.0266287.
[19] K. Zhao, M. Zhang, J. Ji, R. Zhang, J.M. Bewley, Automatic lameness scoring of dairy cows based on the analysis of head- and back-hoof linkage features using machine learning methods, Biosys. Eng. 230 (2023) 424–441, https://doi.org/10.1016/J.BIOSYSTEMSENG.2023.05.003.
[20] A. Poursaberi, C. Bahr, A. Pluk, A.V. Nuffel, D. Berckmans, Real-time automatic lameness detection based on back posture extraction in dairy cattle: shape analysis of cow with image processing techniques, Comput. Electron. Agric. 74 (1) (2010) 110–119, https://doi.org/10.1016/J.COMPAG.2010.07.004.
[21] K. Zhao, J.M. Bewley, D. He, X. Jin, Automatic lameness detection in dairy cattle based on leg swing analysis with an image processing technique, Comput. Electron. Agric. 148 (2018) 226–236, https://doi.org/10.1016/J.COMPAG.2018.03.014.
[22] Ma, H., Chen, L., Kong, D., Wang, Z., Liu, X., Tang, H., Yan, X., Xie, Y., Lin, S.-Y., & Xie, X. (2021). TransFusion: cross-view fusion with transformer for 3D human pose estimation. *ArXiv*. https://doi.org/10.48550/arXiv.2110.09554.
[23] Wang, J., Sun, K., Cheng, T., Jiang, B., Deng, C., Zhao, Y., Liu, D., Mu, Y., Tan, M., Wang, X., Liu, W., & Xiao, B. (2019). *Deep high-resolution representation learning for visual recognition* (Version 2). arXiv. https://doi.org/10.48550/ARXIV.1908.07919.
[24] S.J. Maybank, O.D. Faugeras, A theory of self-calibration of a moving camera, Int. J. Comput. Vis. 8 (2) (1992) 123–151, https://doi.org/10.1007/bf00127171.
[25] E.R. Davies, The dramatically changing face of computer vision. Advanced Methods and Deep Learning in Computer Vision, Elsevier, 2022, pp. 1–91, https://doi.org/10.1016/b978-0-12-822109-9.00010-2. ISBN 9780128221099.
[26] O. Moliner, S. Huang, K. Astrom, Better prior knowledge improves human-pose-based extrinsic camera calibration, in: 2020 25th International conference on pattern recognition (ICPR), 2021, pp. 4758–4765, https://doi.org/10.1109/ICPR48806.2021.9411927.
[27] A. Kroese, M. Alam, E. Hernlund, D. Berthet, L.-M. Tamminen, N. Fall, N. Högberg, 3D pose estimation to detect posture transition in free-stall housed dairy cows, J. Dairy Sci. 107 (9) (2024), https://doi.org/10.3168/jds.2023-24427.
[28] W. Hamäläinen, M. Järvinen, P. Martiskainen, J. Mononen, November). Jerk-based feature extraction for robust activity recognition from acceleration data, in: 11th International Conference on Intelligent Systems Design and Applications, 2011, https://doi.org/10.1109/ISDA.2011.6121760.
[29] L. Riaboff, S. Poggi, A. Madouasse, S. Couvreur, S. Aubin, N. Bédère, E. Goumand, A. Chauvin, G. Plantier, Development of a methodological framework for a robust prediction of the main behaviours of dairy cows using a combination of machine learning algorithms on accelerometer data, Comput. Electron. Agric. 169 (2020) 105179, https://doi.org/10.1016/J.COMPAG.2019.105179.
[30] P. Virtanen, R. Gommers, T.E. Oliphant, M. Haberland, T. Reddy, D. Cournapeau, E. Burovski, P. Peterson, W. Weckesser, J. Bright, S.J. van der Walt, M. Brett, J. Wilson, K.J. Millman, N. Mayorov, A.R.J. Nelson, E. Jones, R. Kern, E. Larson, Y. Vázquez-Baeza, SciPy 1.0: fundamental algorithms for scientific computing in Python, Nat. Methods 17 (3) (2020) 261–272, https://doi.org/10.1038/s41592-019-0686-2.
[31] K. Ren, M. Alam, P.P. Nielsen, M. Gussmann, L. Rönnegård, Interpolation methods to improve data quality of indoor positioning data for dairy cattle, Front. Animal Sci. 3 (2022), https://doi.org/10.3389/fanim.2022.896666.
[32] N. Dirksen, L. Gygax, I. Traulsen, B. Wechsler, J.-B. Burla, Body size in relation to cubicle dimensions affects lying behavior and joint lesions in dairy cows, J. Dairy Sci. 103 (10) (2020) 9407–9417, https://doi.org/10.3168/jds.2019-16464.
[33] R. Killick, P. Fearnhead, I.A. Eckley, Optimal detection of changepoints with a linear computational cost, J. Am. Stat. Assoc. 107 (500) (2012) 1590–1598, https://doi.org/10.1080/01621459.2012.737745.
[34] C. Truong, L. Oudre, N. Vayatis, Selective review of offline change point detection methods, Signal Proces. 167 (2020) 107299, https://doi.org/10.1016/J.SIGPRO.2019.107299.
[35] L. Buitinck, G. Louppe, M. Blondel, F. Pedregosa, A. Mueller, O. Grisel, V. Niculae, P. Prettenhofer, A. Gramfort, J. Grobler, R. Layton, J. Vanderplas, A. Joly, B. Holt, G. Varoquaux, API design for machine learning software: experiences from the scikit-learn project, arXiv. (2013), https://doi.org/10.48550/ARXIV.1309.0238.
[36] S.P. Brouwers, A.F.E. Schug, M. Simmler, P. Savary, The effect of neck strap positioning relative to dairy cow body size on rising, lying down, and defecation behaviour in lying cubicles, Animal (2025) 101507, https://doi.org/10.1016/j.animal.2025.101507.
[37] A. Kroese, N. Högberg, D. Berthet, L.-M. Tamminen, N. Fall, M. Alam, Exploring the link between cow size and sideways lunging using 3D pose estimation, in: 11th European Conference on Precision Livestock Farming, 2024, pp. 32–39. https://www.diva-portal.org/smash/record.jsf?pid=diva2%3A1916993&dswid=7796.
[38] K. Nordlund, A flowchart for evaluating dairy cow free stalls, Bovine Practitioner 37 (2) (2003), 89–87.
[39] J.M. Bewley, L.M. Robertson, E.A. Eckelkamp, A 100-year review: lactating dairy cattle housing management, J. Dairy Sci. 100 (12) (2017) 10418–10431, https://doi.org/10.3168/JDS.2017-13251.
[40] U. Schnitzer, Abliegen, liegestellungen und aufstehen beim rind im hinblick auf die entwicklung von stalleinrichtungen für Milchvieh, Kuratorium Für Technik Und Bauwesen in Der Landwirtschaft-Bauschriften 10 (1) (1971) 43.